Quantification of uncertainty on the catalytic property of reusable thermal protection materials from high enthalpy experiments

Francois Sanson, Nadège Villedieu, Francesco Panerai, Olivier Chazot, Pietro Marco Congedo, Thierry E. Magin

Quantification of uncertainty on the catalytic property of reusable thermal protection materials from high enthalpy experiments

Francois Sanson[a], Nadège Villedieu[b], Francesco Panerai[b,1,*], Olivier Chazot[b], Pietro M. Congedo[a], Thierry E. Magin[b]

[a]*INRIA Bordeaux Sud-Ouest, 200 Rue de la Vieille Tour, 33405 Talence, France*
[b]*von Karman Institute for Fluid Dynamics, Chaussée de Waterloo 72, 1640 Rhode-Saint-Genèse, Belgium*

Abstract

An accurate determination of the catalytic property of thermal protection materials is crucial to design reusable atmospheric entry vehicles. This property is determined by combining experimental measurements and simulations of the reactive boundary layer near the material surface. The inductively-driven Plasmatron facility at the von Karman Institute for Fluid Dynamics provides a test environment to analyze gas-surface interactions under effective hypersonic conditions. In this study, we develop an uncertainty quantification methodology to rebuild values of the gas enthalpy and material catalytic property from Plasmatron experiments. A non-intrusive spectral projection method is coupled with an in-house boundary-layer solver, to propagate uncertainties and provide error bars on the rebuilt gas enthalpy and material catalytic property, as well as to determine which uncertainties have the largest contribution to the outputs of the experiments. We show

*Corresponding author. Tel.: +32 2 359 96 00
Email address: panerai@vki.ac.be (Francesco Panerai)
[1]Current address: AMA Inc. at NASA Ames Research Center, Mail Stop 234-1, Moffett Field, CA 94035, USA

that the uncertainties computed with the methodology developed are significantly reduced compared to those determined using a more conservative engineering approach adopted in the analysis of previous experimental campaigns.

Keywords: Uncertainty Quantification, Catalysis, Thermal Protection Systems

---

1. Introduction

Many achievements in rocket science have been made since Apollo, but the prediction of the heat flux to the surface of spacecraft remains an imperfect science, and inaccuracies in these predictions can be fatal for the crew or the success of exploration missions. This quantity is estimated during the design phase of the heat shield used to protect payload and astronauts during the spacecraft atmospheric entry. Predicting the heat flux with accuracy is a rather involved exercise, due to complex multi-physics phenomena typical of hypersonic flows, in particular gas-surface interactions. In order to properly size a Thermal Protection System (TPS) and verify design margins, nominal values determined from ground testing are required, and also their associated uncertainties. It is difficult to rigorously quantify "error bars" on heat-flux predictions. Usually, engineers resort to safety factors to determine the heat shield thickness. This approach is often too conservative, at the expense of a reduced mass of the embarked payload, whereas it can also lead in some conditions to "lucky" heat shield design with barely enough safety margins. Some famous examples are the design of Apollo, Galileo, and Huygens TPS [1].

As opposed to safety factors, Uncertainty Quantification (UQ) is a more systematic approach to establish the variability of a given quantity of interest (QOI) due to the system uncertainties. At the interface of physics, mathematics, and

statistics, UQ tools aim at developing rigorous methods to characterize the impact of "limited knowledge" on a QOI such as the heat flux. This limited knowledge arises from uncertainties related to the inputs of any computation attempting to represent a physical system. The uncertainties are naturally associated to the choice of the physical models and to the specification of the input parameters required for performing the analysis. As an example, numerical simulations require the precise specification of boundary conditions and typically only limited information is available from corresponding experiments. Note that numerical errors associated to the translation of a mathematical formulation into a numerical algorithm (and a computational code) are not considered here as uncertainties (see [2] for more details).

Several examples of UQ techniques (Monte Carlo sampling, Polynomial Chaos, Bayesian methods, etc.) applied to the analysis of complex multiphysics experiments/simulations can be found in the literature [3–5]. Upadhyay [3] *et al.* used a Bayesian method to quantify the uncertainty of a laboratory reactor experiment, investigating the nitridation of graphite. Using UQ, the authors obtained a larger reaction efficiency than that deterministically obtained from the modeling of the experimental setup. Reference [4] documents an uncertainty quantification analysis of ignition times in H_2/O_2 mixtures, determined from computations and shock-tube experiments. The authors used Monte Carlo sampling to show an increase in the contribution of H-impurities at higher dilution and lower pressures, as well as a negligible effect of kinetic uncertainties compared to the H-impurities, except for air at high temperature for which the role of kinetic uncertainties is dominant. A Bayesian method was used by Cheung *et al.* to quantify the uncertainties in the modeling of the $HCN/O_2/Ar$ mixture kinetics.

In this work, we develop an uncertainty quantification methodology to rebuild values of the gas enthalpy and the catalytic property of a reusable TPS material from Plasmatron experiments conducted at the von Karman Institute for Fluid Dynamics (VKI). The knowledge of the catalytic property, often referred to as effective catalytic recombination coefficient or catalycity, is essential for the development of a reusable heat shield. It can be defined as the probability of a flow-surface system to promote recombination reactions of dissociated species that come from the gas phase and diffuse to the wall. Due to the exothermic nature of these reactions, the catalytic property significantly contributes to the heat transferred to the wall. The methodology for characterizing catalytic gas-surface interactions in the VKI Plasmatron facility is based on experimental measurements and their numerical rebuilding using Computational Fluid Dynamics (CFD) simulations. The goal of this paper is to identify the main uncertainties from experiments on ceramic matrix composites [6] and to quantify, based on a non-intrusive spectral projection method, how these uncertainties propagate into the numerical rebuilding of the plasma flow enthalpy and the catalytic property of the TPS material sample. The work is structured in three sections. The first part recalls the main concepts of the methodology used to determine the catalytic properties from Plasmatron experiments. The second section describes the rigourous uncertainty quantification methodology implemented in this study and its novel features compared to a more conservative engineering approach used to compute error bars. The last section presents the results obtained applying the UQ framework to the Plasmatron test campaign.

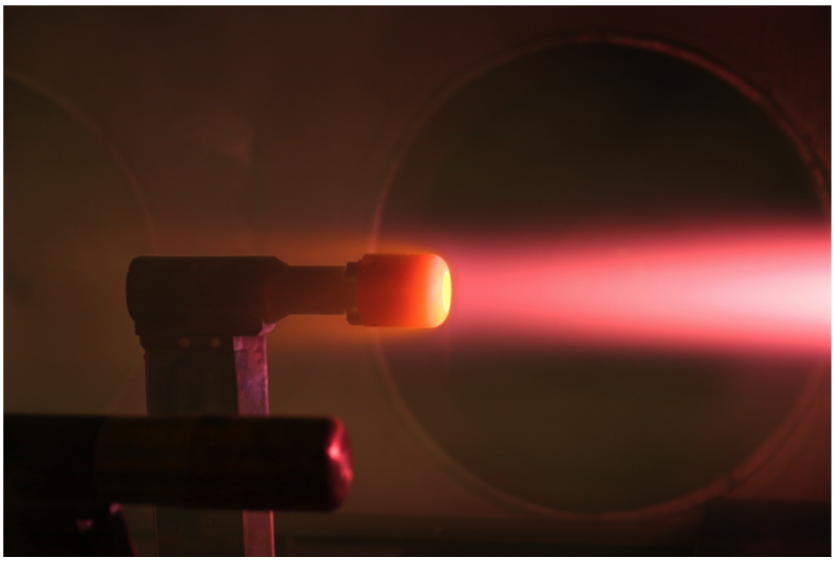

Figure 1: TPS material testing in the VKI Plasmatron facility: stagnation-point probe holding a material sample in plasma jet and calorimetric probe outside of plasma.

2. Enthalpy rebuilding and catalytic property determination

The Plasmatron facility provides an ideal test environment for investigating catalysis effects on TPS materials. The inductively-coupled technology for plasma generation produces an impurity-free flow, ideal to study gas-surface interaction phenomena. Figure 1 shows a typical picture of Plasmatron experiment, where a stagnation-point probe holding a TPS material sample is immersed in the core of a plasma jet and heated to high temperatures. A water-cooled calorimetric probe that is used for calibrating the flow conditions stands in the foreground of the picture.

The Plasmatron facility generates a subsonic, high-enthalpy flow. The testing methodology is based on the simulation of the chemically reacting boundary layer in the stagnation region of a hypersonic body. Aerothermochemical condi-

tions similar to those encountered at hypersonic regimes are reproduced around a representative model of the TPS material. The subsonic-hypersonic similarity can be described by means of the Local Heat Transfer Simulation theory [7–9], which is based on the Fay and Riddell [10] and Goulard [11] formulae for the heat flux at the stagnation point of a body immersed in a chemically reacting flow. Built upon this theory, a methodology has been consolidated at VKI in order to evaluate the catalytic property of a TPS material by combining experimental measurements from the Plasmatron facility and CFD simulations [6, 9, 12], as shown in the schematic in Figure 2. Two steps are involved: the first one aims at calibrating certain flight conditions to be simulated in the experimental facility, the second one aims at determining the catalytic property of the tested material, under these conditions. In Figure 2 the QoIs for the two steps are highlighted in blue. Flight conditions are defined by the boundary-layer edge enthalpy h_e, corresponding to the flight speed, and pressure P_s, corresponding to the flight altitude. The quantity P_s is directly measured, therefore it is not considered to be a QoI, but rather an input uncertainty. The catalytic property of the material surface are described by a global, phenomenological catalytic recombination coefficient γ, which quantifies the amount of catalytic heating transferred to the TPS material surface under the prescribed flights conditions.

The determination of flight conditions, that is the rebuilding of enthalpy h_e at the bounday layer edge, can be summarized in the following steps:

- Plasmatron testing conditions are determined by controlling the gas (air in the cases analyzed herein) mass flow $\dot{m}$, the electrical power PW and the chamber static pressure P_s. The gas mass flow is controlled using a calibrated rotameter. The electrical power dissipated into the plasma is a frac-

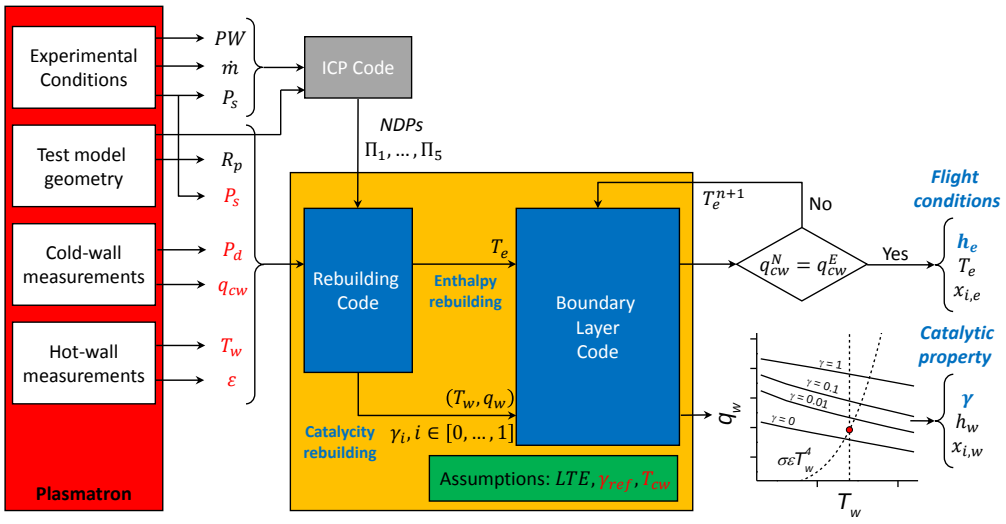

Figure 2: Schematic of enthalpy rebuilding and catalytic property rebuilding methodology.

tion (typically ≈40%) of the generator power setting. The pressure P_s is measured by an absolute pressure gauge and adjusted to the required value by means of vacuum pumps and by-pass flow regulation.

- Testing conditions are calibrated based on cold-wall heat flux q_{cw} measurements, performed with a water-cooled calorimetric probe, and the determination of the total pressure P_{tot} at the TPS sample location. The total pressure is obtained from the dynamic pressure P_d measured by means of a Pitot probe and the static pressure P_s. Both heat flux and Pitot probes have the same geometry (radius R_p) as the TPS probe.

- The following assumptions are made: Local Thermodynamic Equilibrium (LTE) conditions hold at the boundary layer edge [13], the temperature of the water-cooled calorimeter is $T_{cw} \approx 350$ K, and its copper surface has a known catalytic recombination coefficient γ_{ref} of large magnitude (lower

than one) relative to recombination of O and N atoms.

- Magneto-hydrodynamic (MHD), axisymmetric computations of the Plasmatron environment are performed to extract Non-Dimensional Parameters (NDPs) that characterize the plasma flowfield at the edge of the boundary layer. For these simulations, the Plasmatron settings are provided as input conditions (mass flow $\dot{m}$, electrical power PW, and chamber static pressure P_s).

- Stagnation-line flow computations are performed using a chemical non-equilibrium boundary layer code. The code solves non-equilibrium boundary layer equations, yielding the cold-wall, catalytic heat-flux at the calorimetric probe surface q_{cw}. It is iteratively called by a rebuilding code based on Newton's method that iterates over the boundary-layer edge temperature T_e until the computed heat flux is equal to the one measured experimentally. A more detailed explanation is provided in Figure 2. Once the temperature T_e is determined, the flight conditions (enthalpy h_e and pressure P_s) are known, as well as the plasma composition since the LTE assumption holds at the boundary-layer edge.

The determination of the catalytic property γ of the TPS material follows a procedure similar to the rebuilding of the flight conditions. In this case, for solving the stagnation line flowfield, the rebuilt conditions are imposed as boundary condition at the boundary layer edge and hot-wall measurements are used to define the wall boundary conditions. A radiative equilibrium boundary relation is imposed at the wall, equating the incoming heat flux (diffusive + convective contributions) to the one re-radiated by the surface. The heat loss by conduction into

the material is neglected. Measurements at the Plasmatron are performed using a thin-wall TPS sample (∼2-5 mm thickness) backed by a thick refractory insulation (∼3 cm). Steady state is achieved during a test and the back insulation allows to have an equilibrium temperature that limits the heat exchange at the back of the sample, supporting the adiabatic hypothesis. In summary:

- Boundary layer edge conditions are rebuilt following the steps previously described.
- Hot-wall temperature T_w and emissivity ε are measured for a TPS sample model of radius R_p, under the same total pressure P_{tot} and boundary-layer edge enthalpy h_e.
- The rebuilding code identifies the catalytic property γ of the tested TPS surface, by matching the heat flux computed at the wall temperature T_w to the measured value q_w,inferred from the measured temperature and emissivity according to the Stefan-Boltzmann law $q_w = \sigma \epsilon T_w^4$, where quantity σ is the Stefan-Boltzmann constant.

While the described methodology, and analogous reference methods [14, 15], have been extensively applied in the literature [6, 7, 12], the sensitivity of enthalpy rebuilding to a reference catalytic value γ_{ref} is a known and accepted limitation. Other efforts have been devoted to develop alternative methods using subtraction of the convective contribution, obtained from a correlation, from the total measured heat flux [16] or near-surface diagnostic techniques [17].

In the present study, we apply non-intrusive UQ techniques to the rebuilding code coupled with the boundary-layer code. The uncertain inputs to the problem

considered are highlighted in red in Figure 2. We focus on the following uncertain inputs:

- Controlled parameters: static pressure P_s and cold-wall heat flux q_{cw}.
- Measured quantities: dynamic pressure P_d and hot-wall temperature T_w and emissivity ε.
- Assumptions: cold-wall temperature T_{cw} and reference (copper) catalytic property γ_{ref}.

The model geometry is standard and repeated in every test, hence it is not considered as an uncertainty.

3. Determination of error bars

In this section, a methodology is developed to quantify the uncertainties on the QoIs: gas enthalpy h_e and material catalytic property γ. The goal is to understand which are the main uncertain contributions to the values of h_e and γ rebuilt from Plasmatron experiments, rank them, and then compare the error bars calculated by using a UQ method to those obtained based on a more conservative engineering approach. In the following section, the sources of uncertainties are described, then in Section 3.2, the main features of the engineering approach are reviewed, while a more advanced UQ method is presented in Section 3.3.

3.1. Sources of uncertainties

First, let us classify the sources of uncertainty identified in Section 2 [18] into two different categories.

- Experimental data from the Plasmatron are considered *aleatory uncertainties* (variables describing the inherent random nature of the physical system). It is conventional to model these as realizations of a zero mean Gaussian random variable, as the errors come from the accumulation of small errors in the physical system. The variance of that random variable is given by the available error bar from the experimental measurement. The six aleatory variables considered in this study are summarized in Table 1 with their respective relative uncertainty.

Table 1: Distribution of the aleatory variables

Variable	Distribution	Relative uncertainty
P_d [Pa]	Gaussian	6%
P_s [Pa]	Gaussian	4%
q_{cw} [W/m^2]	Gaussian	10%
T_{cw} [K]	Gaussian	10%
T_w [K]	Gaussian	2%
ε [-]	Gaussian	5%

- The wall catalytic property for the reference calorimeteric probe γ_{ref} is treated as *epistemic uncertainty*. The lack of knowledge is ascribed to the complex composition and to the poorly known chemistry of the water-cooled copper surface exposed to an oxygen-rich plasma. A legacy practice [7] consists in assuming that the reference calorimetric probe as fully catalytic (γ_{ref}=1). This provides a conservative catalytic property for the tested TPS material. Nonetheless, studies from both arcjet and induction plasmatron facilities found values on the order of 10^{-2} [13, 19, 20], consistent

with the formation of copper oxides upon exposure to air plasmas. Using X-ray Photoelectron Spectroscopy (XPS), Nawaz et al. [20] documented the formation of cuprous oxide Cu_2O on copper slugs exposed to room air, soon after ($\sim$15 seconds) Wenol® or sandpaper cleaning of the surface. The same authors reported the formation of a thick cupric oxide CuO scale on the slug calorimeters exposed to arcjet airflow for durations as short as 0.3 seconds. The large discrepancies found among values reported in the literature [11, 13, 19–23] justify the classification of γ_{ref} as epistemic uncertainty. In Section 4, we perform an uncertainty analysis at discrete values of γ_{ref} ranging from 0.05 to 1, in order to understand its influence on the QoIs.

Further contributions to uncertainties in the described problem are related to the choice of the models for the plasma reactive flow and for the gas-surface interactions at the TPS wall. There are five categories of modeling uncertainties that can be identified:

- *Non-dimensional parameters*. As explained in section 2 a set of NDPs is used to characterize the hydrodynamics of the plasma flow at the boundary layer edge. These parameters are calculated from thermo-chemical equilibrium solutions of the Plasmatron (torch + test chamber with probe) flow field. For a given inlet swirl angle, the solution depends on the inlet mass flow, the pressure level and the coupled plasma power (which in turn depends on the Plasmatron generator efficiency η) that are used during a certain experiment. In order to properly quantify NDPs uncertainties, UQ techniques shall be applied to the dedicated CFD code that allows to solve the Plasmatron flow field. This is a complex undertaking that would require coping with the complexity of the physical models involved, the computa-

tional cost of MHD simulations and the difficulty in identifying sources of uncertainty to the specific problem. A sensitivity analysis to the NDPs was performed in [24], using a database of multiple CFD simulations at different combinations of static pressure, mass flow and power, within the Plasmatron operating envelope. It was shown that, for a given mass flow and pressure, variations of NPDs computed at generators efficiencies between $\eta = 40$ and 60% yield variations in h_e and γ of less than 0.6%. Based on this analysis, it can be concluded with confidence that NPDs are negligible in the present problem.

- *Thermodynamic and transport properties of the plasma flow*. Since the highest-fidelity models, with the best data currently available in the literature are used [25, 26], thermodynamic and transport models can be considered as certain.

- *Gas chemistry model*. Uncertainties in the gas chemistry model are due to both the number of species used to approximate the test gas, and the selected reaction rates. In [24], a comparison of 5, 7 and 11-species models for air mixture conducted on series of test cases at different pressures, showed that for Plasmatron experiments at relatively low enthalpies ($\lesssim 25$ MJ/kg), both and are nearly insensitive to the number of species. A small sensitivity (on the order of ≈5%) was observed for γ_{ref} values below 10^{-3}, which however are highly unlikely. A similar behavior was observed when changing from the baseline Dunn and Kang [27], rates to those of Park [28] and Chung [29]

- *Surface chemistry model*. The boundary layer code used in the present study adopts a very simplified engineering model that accounts for only O and N-

atom recombination into O_2 and N_2, respectively, at equal rates. Nitric oxide production, which was demonstrated to occur on quartz surfaces [30, 31] from room temperature to 1200 K, is not included. Oxidation reactions, which are fundamental to the analysis of silica forming surfaces as those in [6], are also not modeled. Moreover, the model assumes full energy accommodation to the surface. These approximations are indisputably sources of uncertainty to the analysis of Plasmatron experiments. Several, more advanced surface reaction models have been developed for CFD simulations and the work by Marschall et al. [32] is a comprehensive reference on the topic. The challenge in applying advanced finite-rate catalysis formulations lies into the availability of high-fidelity recombination coefficients and, when those are available from controlled laboratory experiments, their applicability to more complex environments like the Plasmatron or even a real flight environment. This is still an open field of investigation, and dedicated, future study shall be devoted to quantify the uncertainties of surface chemistry models.

- *Boundary-layer edge thermo-chemical state*. Local thermo-chemical equilibrium (LTE) conditions are assumed at the boundary-layer edge. This assumption has been validated using spectroscopy measurements [13] for the test conditions analyzed in the present work. Recent numerical investigations [33] suggest nonetheless that LTE may not hold under different conditions (e.g. lower mass flows). In such a circumstance this shall be considered as an additional source of uncertainty.

As we intend to focus on experimental uncertainties and on how they propagate through the rebuilding procedure, the listed modeling uncertainties are ne-

glected. Their influence shall be further studied in a dedicated UQ analysis beyond the scope of the present study.

3.2. Engineering approach

In [12], Marschall *et al.* showed independent effects of temperature T_w, hot wall heat flux q_w (emissivity) and enthalpy h_e on the final value of the catalytic property γ. A $\pm 10\%$ assumption on the relative uncertainty of h_e was adopted, emissivity ε uncertainties were taken as +0.1/-0.2 and the measurement error on the temperature was set to the quoted instrument uncertainty. Uncertainties on the calorimetric probe catalytic property γ_{ref} and wall temperature T_{cw} were neglected, and each input uncertain variable was considered separately.

Following this approach, variability ranges for enthalpy and catalytic property values from Plasmatron experiments can be computed. Below, the technique is applied to a reference case (sample S12 in [6], $q_{cw} = 735$ W/m^2, $P_s = 2010$ Pa, $T_w = 1600$ K) used in the following sections to determine error bands for both QoIs h_e and γ:

- Nominal (measured) values of heat flux, static pressure, dynamic pressure and, wall temperature and emissivity are denoted as q^*_{cw}, P^*_s , P^*_d, T^*_w and ε^*, respectively.

- The Δ uncertainty on each variable is based on the values reported in Table 1 and defines upper and lower limits for the variable, which are denoted with the superscripts *, $^+$ and $^-$, respectively. For example, for a wall temperature T_w of 1600 K and $\Delta T_w = 2\%$ relative uncertainty, the upper and the lower values are $T^-_w = 1568$ K and $T^+_w = 1632$ K, respectively.

- The numerical rebuilding detailed in Section 2 is performed for the nominal, lower and upper value of each variable, the others being fixed to their nominal value for each simulation.

A summary of the results obtained for the sample S12 from [6] is provided in Table 2. Upper and lower margins are highlighted in red and blue respectively. As expected, one can notice that higher values of enthalpy h_e result from a positive relative uncertainty on the heat flux q_{cw}^+, and negative relative uncertainty on the static and dynamic pressures, P_s^- and P_d^-. The dissociation of a plasma is enhanced at lower pressures P_s, its enthalpy being higher. Assuming a constant total enthalpy, a lower dynamic pressure results in a higher static enthalpy. Similarly, lower values of enthalpy h_e are given by the bounds q_{cw}^-, P_s^+ and P_d^+. Obviously, the enthalpy does not depend on the hot wall temperature T_w and emissivity ε, which are properties of the sample.

Lower values of the TPS catalytic property are given by the bounds q_{cw}^+, P_s^+, P_d^+, T_w^-, and ε^-. For a positive error in q_{cw}, a higher wall heat flux is obtained at a given surface catalytic property and at given temperature (in the q_w versus T_w plot in Figure 2 the iso-γ curves shift upwards). Therefore, for the same sample temperature and emissivity, a lower γ is obtained from the rebuilding. Similarly, for a negative error on the wall temperature T_w or on the emissivity ε, the re-radiated heat flux is lower, hence a lower γ is determined.

In order to estimate the final error bar a further rebuilding is performed combining the marginal inputs giving a similar effect, therefore yielding the highest and lowest possible values for each QoI. The computed error bars $\Delta h_e = [h_e^-, h_e^+]$ for the enthalpy and $\Delta\gamma = [\gamma^-, \gamma^+]$ are shown in Table 3.

Table 2: Rebuilt values of the QoI based on engineering approach for reference case (sample S12 in [6], $q_{cw} = 735$ W/m^2, $P_s = 2010$ Pa, T_w = 1600 K). Enthalpy values are rebuilt with a T_{cw} = 350 K surface temperature value. Variation of h_e due to T_{cw} are negligible, hence they are not included.

Input variable	Enthalpy h_e [MJ/kg]	Catalytic property γ
P_s^*	16.70	0.00862
P_s^-	16.92	0.009603
P_s^+	16.49	0.00823
P_d^*	16.70	0.00862
P_d^-	16.94	0.00868
P_d^+	16.47	0.00855
q_{cw}^*	16.70	0.00862
q_{cw}^-	15.04	0.00862
q_{cw}^+	18.38	0.00712
T_w^*	–	0.00862
T_w^-	–	0.00737
T_w^+	–	0.00997
ε^*	–	0.00862
ε^-	–	0.00719
ε^+	–	0.01013

Table 3: Maximum and minimum values of h_e and γ based on engineering approach for reference case (sample S12 in [6], $q_{cw} = 735$ W/m^2, $P_s = 2010$ Pa, T_w = 1600 K)

QoI and input combination	Value
$h_e^- = h_e^-(q_{cw}^-, P_s^+, P_d^+)$	14.66 MJ/kg
$h_e^+ = h_e^+(q_{cw}^+, P_s^-, P_d^-)$	18.92 MJ/kg
$\gamma^- = \gamma^-(q_{cw}^+, P_s^+, P_d^+, T_w^-, \varepsilon^-)$	0.00457
$\gamma^+ = \gamma^+(q_{cw}^-, P_s^-, P_d^-, T_w^+, \varepsilon^+)$	0.01522

3.3. Uncertainty quantification method

In this section, the generalized Polynomial Chaos (gPC) method is presented as a rigorous UQ method for computing error bars on the QoIs for the described problem. It was originally developed by [34]. The gPC stochastic expansion provides with a method to build a polynomial approximation of a function of stochastic variables. Let us define f as the square integrable function of interest that takes the random vector $(\xi_1, \xi_2, \xi_3, ..\xi_n)$ of n known distributions as input, n being the dimension of the input space. The generalized polynomial chaos (gPC) theory asserts that f can be approximated by an orthogonal polynomial with respect to the input space $(\Xi, p_{\xi_1,\xi_2,\xi_3,..\xi_n})$, with a converging error in the mean-square sense [35]. The classical gPC construction provides us with with a polynomial of order N denoted as $P_N(\xi_1, \xi_2, \xi_3, ..\xi_n)$, i.e.

$$f(\xi_1, \xi_2, \xi_3, ..\xi_n) \simeq P_N(\xi_1, \xi_2, \xi_3, ..\xi_n) = \sum_i \alpha_i \Psi_i(\xi_1, \xi_2, \xi_3, ..\xi_n). \qquad (1)$$

Here, Ψ_i is the polynomial basis, which is orthogonal with respect to the probability measure associated to the uncertain inputs. For Gaussian distributed uncertainties, the polynomial basis is built using the tensorisation of n one-dimensional Hermitian polynomials (six in the present case). Besides $L_2(\Xi, p_{\xi_1,\xi_2,\xi_3,..\xi_n})$, the

space of square integrable functions is a Hilbert space with the following scalar product:

$$\langle u, v \rangle = \int_{\Xi} u(\xi_1, \xi_2, \xi_3, ..\xi_n) v(\xi_1, \xi_2, \xi_3, ..\xi_n) p(\xi_1, \xi_2, \xi_3, ..\xi_n) d\xi_1 d\xi_2 d\xi_3 .. d\xi_n, \tag{2}$$

where $p(\xi_1, \xi_2, \xi_3, ..\xi_n)$ is the product of n one dimensional Gaussian distributions. Then, it follows that

$$\langle \Psi_i, \Psi_j \rangle = \langle \Psi_i, \Psi_i \rangle \delta_{i,j}, \tag{3}$$

for any i and j. In order to compute α_i, the orthogonality property from Eq. 3 can be used by projecting f on each component of the basis. From Eq. 1 it follows that

$$\alpha_i = \frac{\langle f(\xi_1, \xi_2, \xi_3, ..\xi_n), \Psi_i(\xi_1, \xi_2, \xi_3, ..\xi_n) \rangle}{\langle \Psi_i, \Psi_i \rangle}. \tag{4}$$

Therefore the computation of $P_N(\xi_1, \xi_2, \xi_3, ..\xi_n)$ consists in computing the α_i and therefore evaluating an integral according to Eq. 4. In our case, we used the Hermite Gauss quadrature rule described in [35]. As no modifications to the deterministic code computing f are needed, the method is non intrusive. Only evaluations of the function at several collocation points are required for the quadrature rule.

In order to evaluate the results of the gPC analysis, the Sobol indices [36] can be computed to study the sensitivity of $f(\xi_1, \xi_2, \xi_3, ..\xi_n)$ to each random variables. Sobol indices compare the variance of the conditional expectation $Var_{\xi_i}[E(y|\xi_i)]$ against the total variance $Var(y)$, where E denotes the expected value. The Sobol index S_i for the variable ξ_i is defined as:

$$S_i = \frac{Var_{\xi_i}[E(y|\xi_i)]}{Var(y)}. \tag{5}$$

Sobol indices quantify the contribution of each source of uncertainty to the variance of the ouputs. Once the coefficient of the polynomial are computed, the

statistical moments of $f(\xi_1, \xi_2, \xi_3, ..\xi_n)$ and the Sobol indices are readily available from the coefficients of the polynomial [35]. The built polynomial provides a cheap metamodel that can be evaluated multiple times at low computational cost, enabling to rebuild an estimation of the Probability Distribution Function (PDF) and Cumulative Distribution (CDF) of the output.

In the next section, the results obtained with the gPC are presented. While not reported here, the convergence of the stochastic method is systematically checked for each one of the cases analyzed. In particular, an increasing polynomial order is considered, showing that orders 2 and 3 are always sufficient to attain convergence. Both expansions yield very accurate results at the quadrature points where the actual function is evaluated, thus validating the statistics estimation.

4. Results

In this section, we present the results obtained based on the gPC theory. First, the influence of the reference catalytic property γ_{ref} on the resulting uncertainty on the TPS sample catalytic property γ is discussed. Eleven values of γ_{ref} ranging from 0.05 to 1 are selected, and the uncertainty analysis is carried out at those points for one exemplary condition corresponding to case S8 in [6] ($q_{cw} = 410$ W/m^2, $P_s = 3020$ Pa, T_w = 1400 K). Later the influence of the mean measured quantities on the rebuilt gas enthalpy h_E and material catalytic property γ are discussed for several test cases from [6].

4.1. Study of the influence of reference catalytic property γ_{ref} for reference case (sample S8 in [6], $q_{cw} = 410$ W/m^2, $P_s = 3020$ Pa, T_w = 1400 K)

Figures 3 and 4 show the influence of the reference probe catalytic property γ_{ref} on the QoIs based on both the PDF and CDF of h_e and γ. It is observed

that the reference probe catalytic property has a significant influence on the mean reconstructed values of the QoI. For the specific case illustrated, we computed a reduction in the boundary layer edge enthalpy of nearly 10%, from $h_e \approx 10.2$ to ≈ 9.3 MJ/kg, while increasing γ_{ref} from 0.05 to 1. Similarly, the rebuilt catalytic property doubles from $\gamma = 0.0028$ to 0.006 for γ_{ref} increasing from 0.05 to 1.

The mean values for the rebuilt quantities are presented in Figure 5 with $\mp\sigma$ error bars, for increasing γ_{ref}. The plots show that for γ_{ref} values higher than 0.2 there is only a slight variation in the rebuilt quantities. This is a well-know behavior, commonly observed on the "S-shaped" curves that plot the variability of rebuilt quantities with γ_{ref}. An example is provided in Figure 6 for h_e. For a given heat flux value, a lower reference catalytic property yields a higher enthalpy due to the lower effectiveness of the surface in recombining atoms [37]. The "S-shaped" plot highlights that for a nearly non-catalytic reference surface ($\gamma_{\text{ref}} \lesssim 10^{-4}$), or a nearly fully-catalytic one ($\gamma_{\text{ref}} \gtrsim 10^{-1}$), there is a very small variation on the rebuilt h_e. Conversely for partial reference catalycity values, a small variation in γ_{ref} produces a large variation in the rebuilt quantities.

Figure 5 also highlights that the probe catalytic property not only influences the mean rebuilt QoI, but it also affects their uncertainty. Interestingly, it is observed that, in the region where γ_{ref} has a larger influence ($\gamma_{\text{ref}} \lesssim 2 \cdot 10^{-1}$), the uncertainties in the experimental measurements produce smaller error bars. This effect is more pronounced for γ, where clearly smaller error bars are observed for $\gamma_{\text{ref}} < 0.2$.

In order to further investigate the influence of each experimental uncertainty on the QoI error bars, the Sobol indices of the aleatory variables are presented in Figure 7 for the enthalpy, and in Figure 8 for the sample catalytic property, at

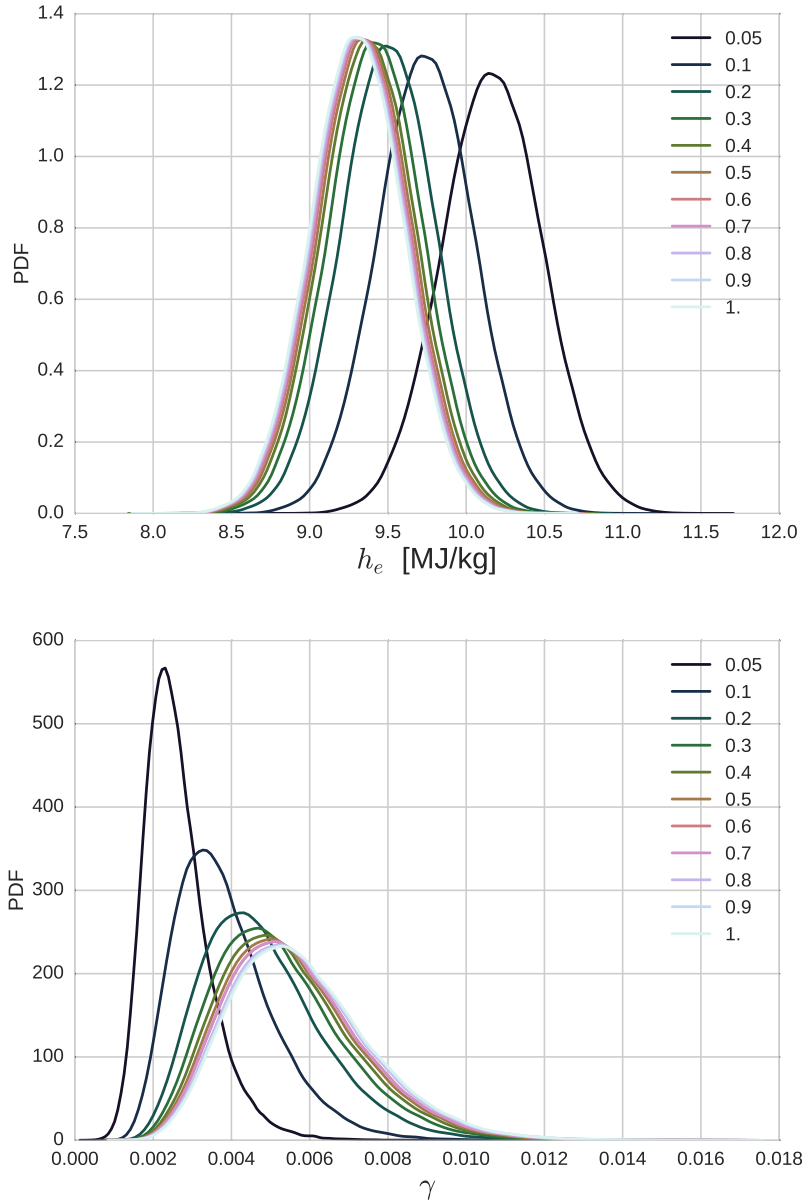

Figure 3: Evolution of the PDF for the rebuilt gas enthalpy h_e (top) and material catalytic property γ (bottom), as a function of the reference material catalytic property γ_{ref} for reference case (sample S8 in [6], $q_{cw} = 410$ W/m^2, $P_s = 3020$ Pa, T_w = 1400 K).

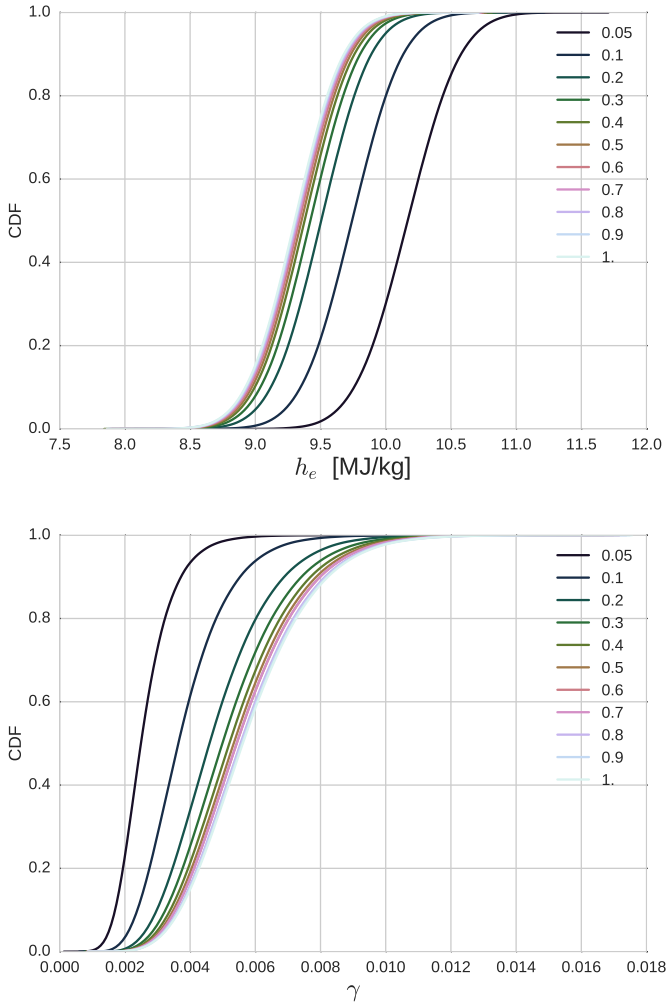

Figure 4: Evolution of the CDF for the rebuilt gas enthalpy h_e (top) and material catalytic property γ (bottom) as a function of the reference material catalytic property γ_{ref} for reference case (sample S8 in [6], $q_{cw} = 410$ W/m^2, $P_s = 3020$ Pa, T_w = 1400 K).

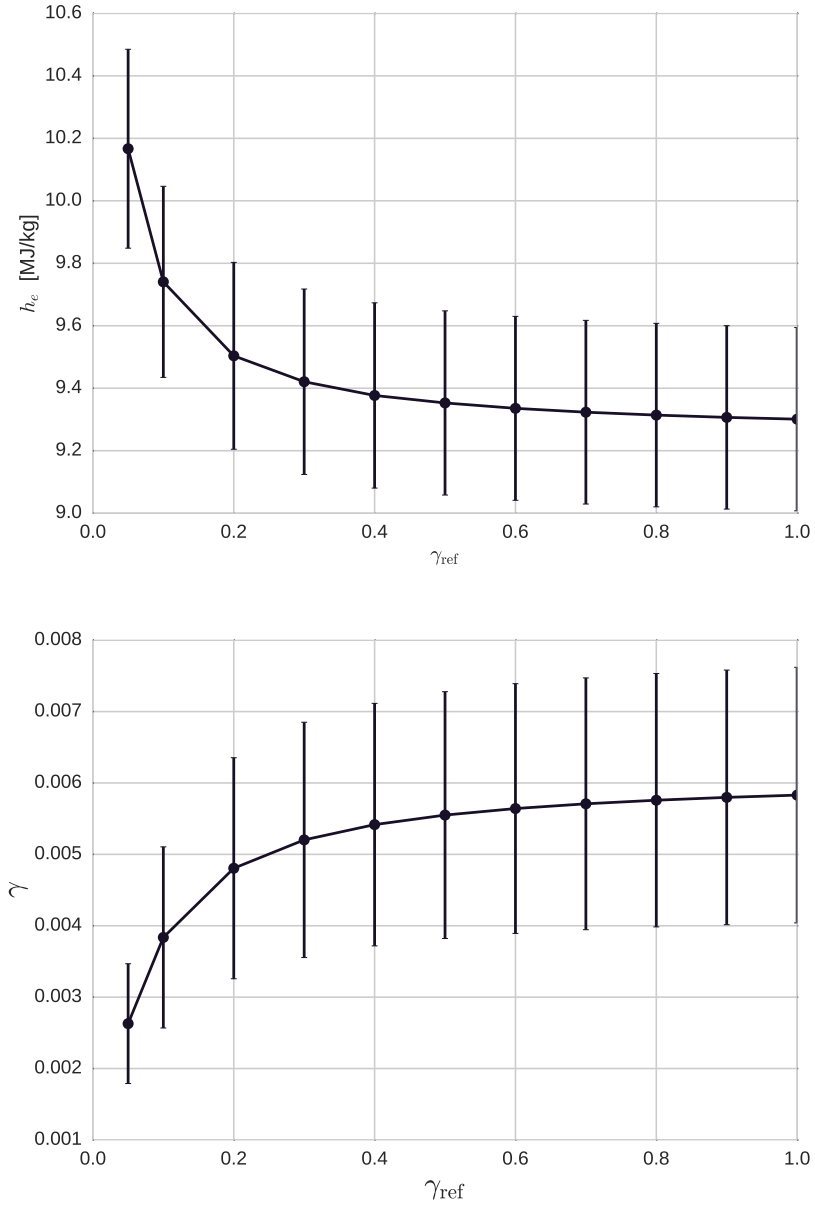

Figure 5: Evolution of the mean values and 2σ error bars for the rebuilt gas enthalpy h_e (top) and material catalytic property γ (bottom) as a function of the reference material catalytic property γ_{ref} for reference case (sample S8 in [6], $q_{cw} = 410$ W/m^2, $P_s = 3020$ Pa, T_w = 1400 K).

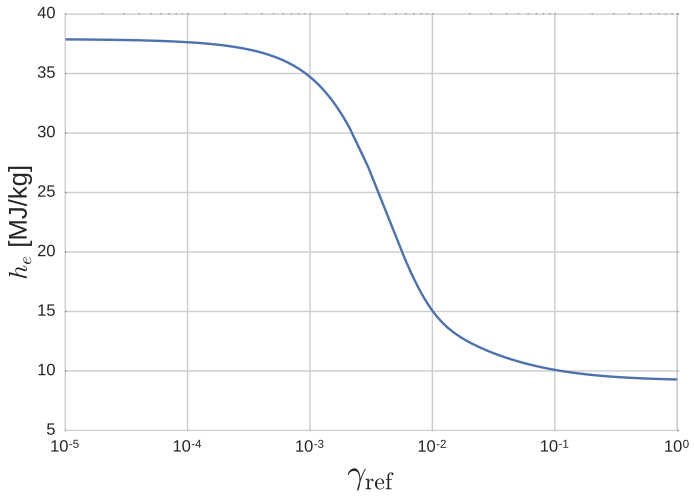

Figure 6: Rebuilt gas enthalpy h_e as a function of the reference material catalytic property γ_{ref} for reference case (sample S8 in [6], $q_{cw} = 410$ W/m^2, $P_s = 3020$ Pa, T_w = 1400 K).

different values of γ_{ref}. As explained in section 3.3, the Sobol indices are good metrics to quantify the system sensitivity to the input uncertainty. It is interesting to observe that the rebuilt gas enthalpy h_e uncertainty is almost exclusively determined by the error in the measured heat flux q_{cw}, which accounts for 97% of the total error at any γ_{ref}. Dynamic pressure P_d and cold-wall temperature T_{cw} measurements have only a minor influence on h_e. Due to the nearly exclusive contribution of wall heat flux to the total uncertainty in h_e, we note that the rebuilt enthalpy distribution is close to a Gaussian distribution.

Similarly, the sample catalytic property γ uncertainty is significantly affected by the cold-wall heat flux q_{cw} (80% of the error). The emissivity ε and temperature T_w of the test sample, that define the re-radiated heat flux from the surface, account for the remaining 20% of the error. Unlike in the case of the gas enthalpy, a reduction of the q_{cw} Sobol index for γ is noticed in Figure 8 for low γ_{ref} values.

Therefore, the decrease in uncertainty previously observed in Figure 5, can be explained by the reduced contribution of cold-wall heat flux q_{cw} to the sample catalytic property variance.

Taken as an aggregate, the above observations suggest that improvements in cold-wall heat flux measurements, which are well-known to be challenging in a high enthalpy flow like that of the Plasmatron, would help reducing the overall uncertainty of future experiments in characterizing effective test conditions and materials' catalytic properties.

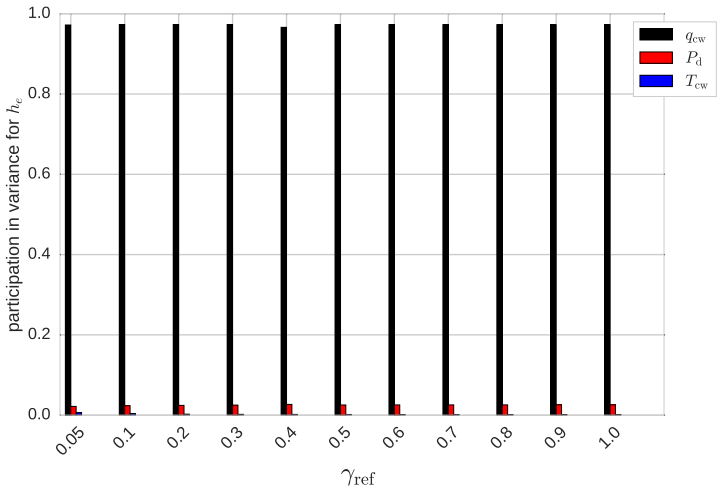

Figure 7: Contribution (Sobol indices) of cold wall heat flux q_{cw}, dynamic pressure P_d, and cold-wall temperature T_{cw} measurements to the uncertainty on the rebuilt gas enthalpy h_e as a function of the reference material catalytic property γ_{ref} for reference case (sample S8 in [6], $q_{cw} = 410$ W/m^2, $P_s = 3020$ Pa, T_w = 1400 K)

.

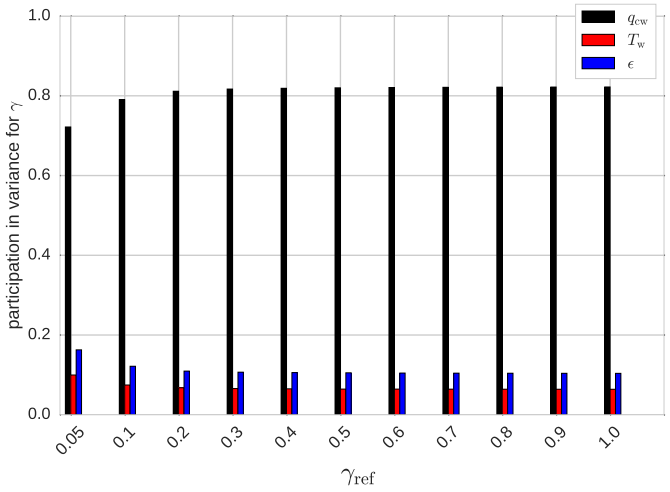

Figure 8: Contribution (Sobol indices) of cold-wall heat flux q_{cw}, hot-wall temperature T_w, and emissivity ε measurements to the uncertainty on the rebuilt material catalytic property γ as a function of the reference material catalytic property γ_{ref} for reference case (sample S8 in [6], $q_{cw} = 410$ W/m^2, $P_s = 3020$ Pa, T_w = 1400 K).

4.2. *Comparison of UQ and engineering approaches for reference case (sample S12 in [6], $q_{cw} = 735$ W/m^2, $P_s = 2010$ Pa, T_w = 1600 K)*

We now compare the error bars obtained based on the UQ methodology to those computed using the engineering approach. As described in section 3, the errors estimated with the engineering approach are defined as the range between the two extreme cases. Using the UQ approach, error bars can be accurately computed, and provided together with the correspondent Confidence Interval (CI). The results are summarized in Table 4, for the same experimental case (S12 from [], $q_{cw} = 735$ W/m^2, $P_s = 2010$ Pa, T_w = 1600 K) analyzed in Table 2. The mean values for the QoIs obtained with both methods are closely similar. For the gas enthalpy h_e, the engineering methodology results in a $\pm 25\%$ accuracy, while the UQ analysis predicts 13% and 17% uncertainty with a confidence level of 95 and 99% respectively. For the catalytic property γ, larger error bars are computed using both methods. This is due the strong non-linearity of the problem, as opposed to the enthalpy that instead varies linearly with the measured heat flux.

Table 4: Comparison of QoI mean values and error bars computed with the engineering and UQ approaches for reference case (sample S12 in [6], $q_{cw} = 735$ W/m^2, $P_s = 2010$ Pa, T_w = 1600 K)

QoI	UQ (mean)	Eng. (mean)	UQ (95% CI)	UQ (99% CI)	Eng. (error bar)
h_e [MJ/kg]	16.75	16.70	13%	17%	25%
γ [-]	0.00867	0.00861	39%	51%	122%

As shown in Figure 9, in the case of γ rebuilding the engineering approach performs poorly by overestimating the uncertainty of more than one order of magnitude. The UQ analysis predicts 39% and 51% uncertainty with a confidence level of 95 and 99%, respectively. The example underlines the need of a rigorous UQ

method for accurately propagating experimental uncertainties through the rebuilding code.

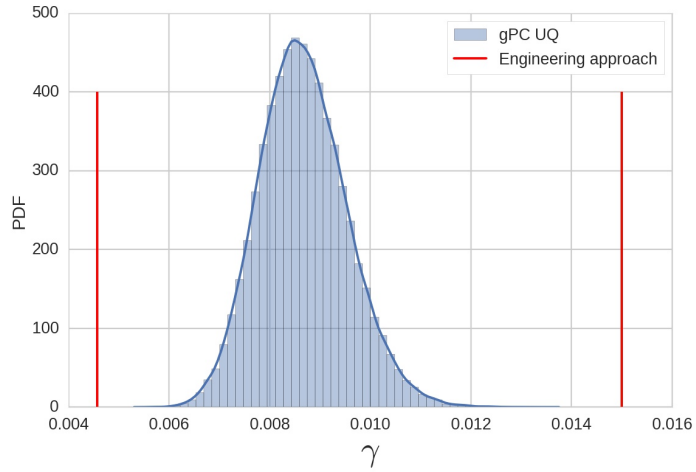

Figure 9: Comparison between the engineering approach and the gPC based UQ approach for the catalytic property γ rebuilding problem.

4.3. Study of cases matrix for fixed reference catalytic property γ_{ref}

In this section, a more detailed sensitivity analysis is carried out in order to provide insight into how the variance decomposition evolves as the experimental conditions change. The six aleatory uncertainties listed in Section 3.3 are considered. As in [6], we make the assumption of a constant reference material catalytic property γ_{ref}= 0.1. Four characteristic cases with experimental conditions given in Table 5 are considered and denoted as a1, a2, a3, and a4. These correspond to case S6 (q_{cw} = 360 W/m^2, P_s = 1320 Pa, T_w = 1400 K), S7 (q_{cw} = 385 W/m^2, P_s = 1980 Pa, T_w = 1400 K), S8 (q_{cw} = 410 W/m^2, P_s = 3020 Pa, T_w = 1400 K) and S12 (q_{cw} = 735 W/m^2, P_s = 2010 Pa, T_w = 1600 K) from [6], respectively.

The first three cases aim at understanding the influence of the static pressure on the contribution to the total variance. For those cases, the static pressure P_s varies from 1320 to 3020 Pa, and the same surface temperature (T_w = 1400 K) is obtained by increasing the cold-wall heat flux q_{cw} for increasing static pressure.

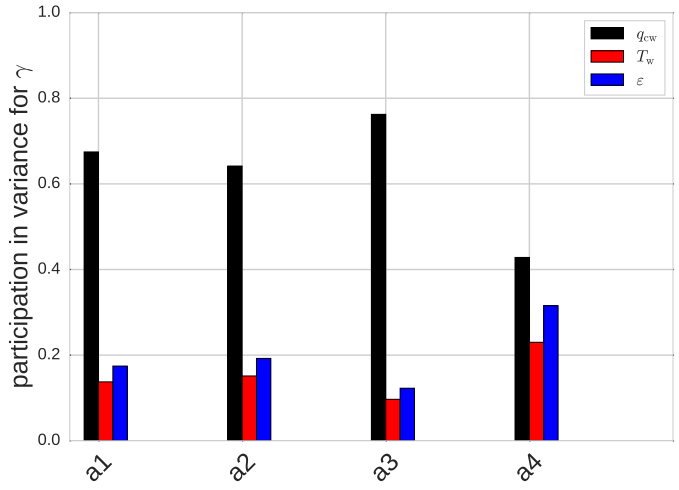

Figure 10: Comparison of the Sobol indices of the cold-wall heat flux q_{cw}, hot-wall temperature T_w, and emissivity ε measurements to the uncertainty on the rebuilt material catalytic property γ for cases a1 to a4.

In Figure 10, the main Sobol indices involved in the determination of the sample catalytic property are plotted. One observes that for a static pressure of 2000 Pa, the contribution of the measured heat flux to the sample catalytic property variance is much lower than for the other conditions. Similarly, the high pressure case is the case where the contribution of the cold-wall heat flux is the highest. This is well explained by the increase in the measurement uncertainty of the heat flux between cases a2 and a3. Case a4 is chosen at a static pressure of P_s = 2000 Pa similar to case a2 but at a higher surface temperature. In this case the contribu-

tion of the three main variables responsible for the catalytic property uncertainty contribute to a similar extent to the total variance. An increase in the sample temperature leads to an increase in the contribution to the sample catalytic property variance from variables measured during the second reconstruction step. Now more than half the variance is explained by the catalytic property rebuilding step. This observation is also correlated with a relatively high sample catalytic property at 8.7e-03. This behavior was not observed for previous cases in this study. This analysis can be extended to more samples and eventually serve as a reference for further experiments. When setting the experimental setup, one could get an estimation about which variable would yield an important contribution being in the vicinity of cases a1, a2, a3 or a4.

5. Conclusion

The uncertainty quantification method is a powerful tool to analyze experimental results. We demonstrated here that the method helps mitigating overconservative error bars computed in TPS characterization when using an engineering approach , that considers in a separate manner the different input variables to the problem. We quantified with 95% confidence a 13% error in the duplication of actual flight condition (boundary layer edge enthalpy) during Plasmatron experiments and an error of $\sim$40% in the computed catalytic property of the reusable TPS material.

The analysis embedded in the gPC method provided understanding of the influence of the measurement error on the QoI. The constructed polynomial approximation can be readily used as a cheap metamodel for rebuilding the QoI PDF.

The documented analysis suggests that, in Plasmatron experiments, the mea-

Table 5: Test conditions and error bars of case a1 to a4. The values are take from case S6, S7, S8 and S12 in [6], respectively

Case	a1 (sample S6 in [6])		a2 (sample S7 in [6])	
	Mean value	Std. Dev.	Mean value	Std. Dev.
P_s [Pa]	1320	17.6	1980	26.4
q_{cw} [W/m^2]	360 000	12 000	385 000	12833.3
P_d [Pa]	83	1.333	60	1.667
T_w [K]	1400	4.667	1400	4.667
ε [-]	0.79	0.01316	0.8	0.01333
T_{cw} [K]	350	11.667	350	11.667
Case	a3 (sample S8 in [6])		a4 (sample S12 in [6])	
	Mean value	Std. Dev.	Mean value	Std. Dev.
P_s [Pa]	3020	40.2	2010	26.8
q_{cw} [W/m^2]	410 000	13 666	735 000	24 500
P_d [Pa]	60	2	115	2.33
T_w [K]	1400	4.667	1600	5.33
ε [-]	0.88	0.01466	0.85	0.01466
T_{cw} [K]	350	11.667	350	11.667

sured cold-wall heat flux is the chief contributor to the rebuilt enthalpy. The reconstruction of the PDF showed that the enthalpy is nearly Gaussian distributed. This behavior comes from the almost linear relationship between the heat flux and the flow enthalpy. We conclude that, reducing experimental errors in heat flux measurements below 10% would enable matching a desired hypersonic condition with less than 10% uncertainty.

Concerning the catalytic property γ of the TPS material, non-linear trends were observed. The cold wall heat flux and the material's emissivity and temperature were identified as main contributors to the rebuilt values of γ. We found that the cold-wall heat flux has a relative contribution of more that 70% to the computed value of γ at temperatures below 1400 K. For higher temperatures ($>$1600 K) we found an increase in the relative importance of the materials' temperature and emissivity to γ. This suggest that improvements on optical measurements for the detection of surface radiative properties would provide a more accurate estimation of catalytic heating from Plasmatron experiments, particularly at very high temperatures.

Finally, we showed that the catalytic property of the reference material features a significant impact on the QoI determined at the Plasmatron. Experimental and numerical efforts shall be directed at improving techniques that can provide a suitable alternative to copper-base reference probes for the characterization of experimental conditions.

Acknowledgment

Research of T.E.M. was sponsored by the European Research Council Starting Grant #259354. The work was partly supported by the European Space Agency (ESA) General Support Technology Programme (GSTP) "Plasmatron+" (contract #4000105388/12/NL/SFe).

References

[1] C. Park. Frontiers of aerothermodynamics. In *RTO-EN-AVT-162 - Non-Equilibrium Gas Dynamics From Physical Models to Hypersonic Flights*,

2008.

[2] G. Iaccarino. Quantication of uncertainty in ow simulations using probabilistic methods. In *RTO-EN-AVT-162 - Non-Equilibrium Gas Dynamics From Physical Models to Hypersonic Flights*, 2008.

[3] R.R. Upadhyay, K. Miki, O.A. Ezekoye, and J. Marschall. Uncertainty quantification of a graphite nitridation experiment using a bayesian approach. *Experimental Thermal and Fluid Science*, 35(8):1588 – 1599, 2011.

[4] Javier Urzay, Nicolas Kseib, David F. Davidson, Gianluca Iaccarino, and Ronald K. Hanson. Uncertainty-quantification analysis of the effects of residual impurities on hydrogenoxygen ignition in shock tubes. *Combustion and Flame*, 161(1):1 – 15, 2014.

[5] Sai Hung Cheung, Kenji Miki, Ernesto Prudencio, and Chris Simmons. Uncertainty quantification and robust predictive system analysis for high temperature kinetics of hcn/o2/ar mixture. *Chemical Physics*, 475:136 – 152, 2016.

[6] Francesco Panerai and Olivier Chazot. Characterization of gas/surface interactions for ceramic matrix composites in high enthalpy, low pressure air flow. *Materials Chemistry and Physics*, 134(2):597–607, 2012.

[7] A. F. Kolesnikov. Conditions of simulation of stagnation point heat transfer from a high-enthalpy ow. *Fluid Dynamics*, 28(1):131–137, 1993.

[8] P. Barbante. *Accurate and Efficient Modelling of High Temperature Nonequilibrium Air Flows*. PhD thesis, Université Libre de Bruxelles, 2006.

[9] P. F. Barbante and O. Chazot. Flight extrapolation of plasma wind tunnel stagnation region flowfield. *J. Thermophys. Heat Transfer*, 20(3):493–499, 2006.

[10] J. A. Fay and F. R. Riddell. Theory of Stagnation Point Heat Transfer in Dissociated Air. *Journal of Aeronautical Science*, 25(2):73–85, 1958.

[11] R. Goulard. On catalytic recombination rates in hypersonic stagnation heat transfer. *Jet Propulsion*, 28(11):737–745, 1958.

[12] J. Marschall, D. A. Pejaković, W. G. Fahrenholtz, G. E. Hilmas, S. Zhu, J. Ridge, D. G. Fletcher, A. Cem, and J. Thoemel. Oxidation of ZrB_2-SiC Ultrahigh-Temperature Ceramic Composites in Dissociated Air . *Journal of Thermophysics and Heat Transfer*, 23(2):267–278, 2009.

[13] A. Cipullo, B. Helber, F. Panerai, L. Zeni, and O. Chazot. Investigation of freestream plasma flow produced by inductively coupled plasma wind tunnel. *Journal of Thermophysics and Heat Tranfer*, 28(3):381–393, 2014.

[14] C. D. Scott. Catalytic Recombination of Nitrogen and Oxygen on High-Temperature Reusable Surface Insulation. In *15^{th} AIAA Thermophysics Conference*, AIAA 1980-1477, Snowmass, CO, USA, July 1980.

[15] S. Pidan, M. Auweter-Kurtz, G. Herdrich, and M. Fertig. Recombination Coefficients and Spectral Emissivity of Silicon-Carbide-Based Thermal Protection Materials. *Journal of Thermophysics and Heat Transfer*, 19(4):566–571, 2005.

[16] B. Massuti-Ballester, S. Pidan, G. Herdrich, and M. Fertig. Recent catalysis

measurements at {IRS}. *Advances in Space Research*, 56(4):742 – 765, 2015.

[17] DG Fletcher and JM Meyers. Surface catalyzed reaction efficiencies in oxygen plasmas from laser-induced fluorescence measurements. *Journal of Thermophysics and Heat Transfer*, pages 1–11, 2016.

[18] WL Oberkampf and Jon C Helton. Investigation of evidence theory for engineering applications. In *AIAA Non-Deterministic Approaches Forum*, pages 2002–1569, 2002.

[19] C. Park, G.A. Raiche, D.M. Driver, and J. Olejniczak. Comparison of enthalpy determination methods for arc-jet facility. *J. Thermophys. Heat Transfer*, 20(4):672–679, 2006.

[20] Anuscheh Nawaz, David M. Driver, Imelda Terrazas-Salinas, and Steven Sepka. Surface catalysis and oxidation on stagnation point heat flux measurements in high enthalpy arc jets. In *In proceeding of 44th AIAA Thermophysics Conference, 2013, AIAA 2013-3138, San Diego, CA, USA*.

[21] J.W. May and Linnett. Recombination of atoms at surfaces - an effusion method applied to oxigen atom recombination. *Journal of Catalysis*, 7(4):324–341, 1967.

[22] V.A. Bityurin, A.N. Bocharov, D.S. Baranov, A.V. Krasilnikov, V.B. Knotko, and Yu.A. Plastinin. Experimental Study of Flow Parameters and MHD Generator Models at High Frequency Plasmatron. In *15^{th} International Conderence on MHD Energy Conversion and 6^{th} Workshop on Magnetoplasma Aerodynamics*, Moscow, Russia, 2005.

[23] Gisu Park. Oxygen catalytic recombination on copper oxide in tertiary gas mixtures. *Journal of Spacecraft and Rockets*, 50(3):540–555, 2013.

[24] Francesco Panerai. *Aerothermochemistry characterization of thermal protection systems*. PhD thesis, PhD thesis, von Kármán Institute for Fluid Dynamics, 2012.

[25] David Bottin Benoît, Vanden Abeele, Mario Carbonaro, , and Gérard Degrez. Thermodynamic and transport properties for inductive plasma modeling. *Journal of Thermophysics and Heat Transfer*, 13:046412, Oct 1999.

[26] Thierry E. Magin and Gérard Degrez. Transport properties of partially ionized and unmagnetized plasmas. *Phys. Rev. E*, 70:046412, Oct 2004.

[27] M. G. Dunn and Kang. S.-W. Theoretical and Experimental Studies of Reentry Plasmas. Contractor Report 2232, NASA Langley Research Center, Hampton, VA, USA, 1973. Prepared by Cornell Aeronautical Laboratory, Inc., Buffalo, NY,14221.

[28] C. Park. *Nonequilibrium hypersonic aerothermodynamics*. John Wiley & Sons, New York, 1990.

[29] P. M. Chung. Chemically Reacting Nonequilibrium Boundary Layer. *Advances in Heat Transfer*, 2(1):109–270, 1965.

[30] Dušan A Pejaković, Jochen Marschall, Lian Duan, and M Pino Martin. Nitric oxide production from surface recombination of oxygen and nitrogen atoms. *Journal of Thermophysics and Heat Transfer*, 22(2):178–186, 2008.

[31] Dušan A Pejaković, DA Pejaković, J Marschall, J Marschall, L Duan, L Duan, MP Martin, and MP Martin. Direct detection of no produced by high-temperature surface-catalyzed atom recombination. *Journal of Thermophysics and Heat Transfer*, 24(3), 2010.

[32] Jochen Marschall, Matthew MacLean, Paul E. Norman, and Thomas E. Schwartzentruber. *Surface Chemistry in Non-Equilibrium Flows*, pages 239–327. Progress in Astronautics and Aeronautics. American Institute of Aeronautics and Astronautics, Inc., 2015.

[33] W Zhang, A Lani, and M Panesi. Analysis of non-equilibrium phenomena in inductively coupled plasma generators. *Physics of Plasmas (1994-present)*, 23(7):073512, 2016.

[34] Dongbin Xiu and George Em Karniadakis. The Wiener–Askey Polynomial Chaos for Stochastic Differential Equations. *SIAM Journal on Scientific Computing*, 24(2):619–644, January 2002.

[35] O. P. Le Maître and Omar M. Knio. *Spectral Methods for Uncertainty Quantification*. Scientific Computation. Springer Netherlands, Dordrecht, 2010.

[36] G. Tang, G. Iaccarino, and M. S Eldred. Global sensitivity analysis for stochastic collocation expansion. In *In Proceedings of the 51st AIAA/ASME/ASCE/AHS/ASC Structures, Structural Dynamics, and Materials Conference (12th AIAA Non-Deterministic Approaches conference), Orlando, FL, April 12-15, 2010.*

[37] Ihor O Bohachevsky and DF DeSanto. A method for determining catalytic efficiency of surfaces. Technical report, DTIC Document, 1967.